DISCUSSION OF A CRITERIA-BASED METHOD FOR ANALYSIS OF INITIAL FOULING RATE

A. D. Smith[1]
[1] Heat Transfer Research, Inc., P.O. Box 1390, Navasota, TX 77868
aaron.smith@htri.net

ABSTRACT

Use of theory, experimental data, and/or field data are popular methods of deriving models to predict fouling. When assessing initial fouling rate from fouling rig test results, criteria deducted from each test needs to be accounted. It would be useful in a scientific context to state clearly the criteria followed for rate assessments; otherwise, the resulting values may not be easily reproducible. This manuscript focuses on the following criteria for rate assessment of a test rig used at HTRI:

1. Corresponds to the initial test conditions (initial fouling rate)
2. Overcomes the impact of a changing film heat transfer coefficient
3. Represents the fouling rate on a fully covered surface
4. Mitigates the influence of any precursor depletion.

A criteria-based analysis algorithm implemented in computer code to address the above requirements. The methodology follows applying the criteria to the fouling resistance, and its first and second derivatives with respect to time, to identify a subset of data that are eligible for analysis. The use of the trend of the first derivative with respect to the fouling resistance and its extrapolation provided the estimate of the fouling rate at zero fouling resistance. The manuscript presents the development of this technique with supporting arguments and data. Application of the method to a wide variety of fouling trends is illustrated.

INTRODUCTION

The purpose of experimental fouling rigs is to perform well-controlled experiments aimed at understanding and modeling fouling, as well as evaluating methods to mitigate fouling.

The discussion of this paper focuses on crude oil fouling experiments performed at HTRI. Crude oil fouling is a dynamic unsteady phenomenon; the fouling rate is a key metric of interest. For experimental fouling data, the rate is likely to change by several factors. Such factors include transition of fouling on a bare metal to fouling on existing deposit (induction period), the changing fluid and surface conditions due to the fouling layer growth (e.g. surface temperature decrease, shear stress increase, and precursor concentration changes can be experienced based on the test set up and how the experiment is performed). The initial fouling rate is the rate that corresponds to the conditions at the reference point. For each fouling test, researchers apply criteria to select individually a period over which to identify a slope as the reported initial fouling rate. When the applied criteria is unreported, the method is subjective and difficult to reproduce. For example, Fig. 1 illustrates different methods researchers could use to assess the fouling rate. Each approach is sensitive to the time period selected and/or the duration of the fouling tests.

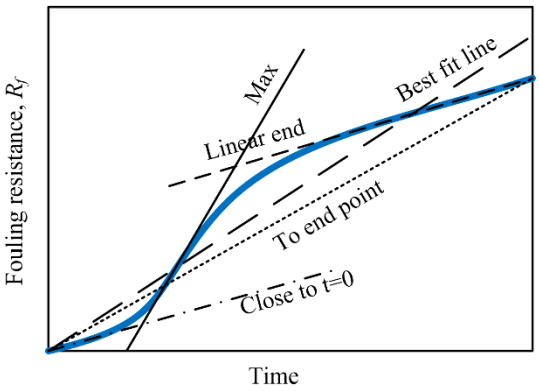

Fig. 1. Illustration of a fouling curve with possible methods used to assess the initial fouling rate.

To avoid arbitrary assessment, some have proposed techniques for consistently determining the fouling rate. Saleh et al. [**1**] used the linear portion of the R_f curve following the induction period which was defined as the point at which the Bi_{Rf} exceeded 0.05 (5% increase in overall resistance to heat transfer). Bennett et al. [**2**] stated rates should be assessed at a point where the fouling rate is positive ($dR_f/dt > 0$) and at the point of the maximum rate ($d^2R_f/dt^2 = 0$). Building on this approach, Smith [**3**] provided criteria created for HTRI crude oil fouling test results to eliminate data that do not exceed a "duration threshold" and/or result from poorly controlled tests. For data that were not discarded, criteria were applied to distinguish those that were "well behaved" (Tier I)

ISBN: 978-0-9984188-1-0; Published online www.heatexchanger-fouling.com

from those that were "not ideal but salvageable" (Tier II). Smith [**3**] applied a smoothing function to Tier 1 data and then assessed the initial fouling rate as the rate at the first point according to the following criteria:

- Time > 0.25 hr
- Rate is greater than the slope of a line from the starting point to the end point
- $R_f > 0$
- $dR_f/dt > 0$
- Fouling increases until end of test ($dR_f/dt > 0$)

The rate for Tier II data was determined from a best-fit line.

Unfortunately, the logical criteria Bennett et al. [**2**] and Smith [**3**] proposed are not supported by data and basic principles of the phenomena occurring at the surface. Further, these methods tend to work only in cases with "well-behaved" fouling curves and minimal amounts of noise.

The proposed method detailed here is based on the observation of a linear trend when fouling rate is plotted vs. fouling resistance. This trend is due to changes in the fluid and initial surfaces conditions that can cause the rate to increase or decrease. For example, in the case of decreasing rate, the surface temperature decreases, shear stress increases, and fouling precursor concentration decreases as the fouling deposit grows. Coupling this observation with data-supported thresholds allowed exclusion of highly uncertain data.

The purpose of this paper is to discuss a framework for development of a fouling rate analysis algorithm (computer code) to analyze HTRI rig data. The method was used to analyze over 100 data sets or experimental runs to obtain initial fouling rate. The proposed method has the potential to be applied to other fouling rigs but would need to be separately evaluated.

OBJECTIVES OF FOULING RATE ANALYSIS

In 2017, Smith et al. [**4**] outlined challenges with interpreting fouling rig data and translating the rig results to field operations. Overcoming these challenges sets the objectives for a fouling rate analysis method. The method described here seeks to incorporate the following objectives:

1. Is implemented as a computer-based algorithm
2. Accounts for impact of changing fluid heat transfer film coefficient
3. Associates fouling rate with the surface conditions
4. Provides fouling rate on deposit rather than metal surface (most meaningful for translation to the field)

Objective 1: Is implemented as a computer-based algorithm

The mandatory requirement is that the analysis method is well defined and implemented in a code. Application of the method is then independent of the user's subjective judgment and applied consistently to all data sets in this study.

Objective 2: Accounts for impact of changing fluid heat transfer film coefficient

The fouling resistance, R_f, is measured by computing the change in the overall heat transfer resistance relative to a reference point [Eq. (1)]. Depending on the type of experiment and the experiment set up, it would be important to account the effect of deposit formation on the convective heat transfer coefficient as discussed by the fouling community [**5**, **6**]. In such examples, it is not valid to assume that the convective heat transfer coefficient remains constant as fouling progresses (i.e., $h = h_{ref}$) and that the measured fouling resistance is the resistance of the deposit (i.e., Eq. (1) reduces to $R_f = R_d$). The deposit constantly affects the convective heat transfer coefficient by reducing the flow path area and changing the roughness of the surface [**5**]. In addition the amount of heat flowing through the test section due to changing end effect (further explained in sections below) needed to be accounted for in electrically heated test sections of short heated length (L/D < 25), which includes HTRI test rigs.

$$R_f = \left(\frac{1}{h} + R_d\right) - \frac{1}{h_{ref}} \tag{1}$$

Smith et al. [**4**] illustrated how a small (1%) change in the heat transfer coefficient can result in significant distortion (> 10%) between the measured fouling resistance, R_f, and the resistance of the deposit, R_d, in the range of typical fouling rig R_f measurements (< 5e-5 m^2 K/W). Actual changes in h are likely much greater that 1%, further increasing this relative error. Therefore, R_f cannot be assumed to be equal to R_d.

Existing methods to model the heat transfer coefficient for single-phase applications are sufficiently accurate (< ± 20 %) [**7**]. What is desired from fouling rig experiments is to understand the rate of the deposit's resistance, R_d. Without methods to assess the true rate of R_d, a large part of what the resulting data (and models fit to those data) may reflect is the change in convective resistance. Thus, this objective to assess a rate that is minimally influenced by the change in convective resistance. This criterion incentivizes measurement of the rate as close to $R_f = 0$; however, this is challenged by the fact that the data near $R_f = 0$ are highly uncertain and therefore should be used, if at all, with caution when analyzing the initial fouling rate.

Objective 3: Associates fouling rate with the surface conditions

Although fouling rigs are typically well controlled, the conditions at the surface of the

ISBN: 978-0-9984188-1-0; Published online www.heatexchanger-fouling.com

deposit change as fouling accumulates. Regardless of the design, the surface temperature generally decreases as fouling accumulates. For electrically powered test sections run at constant duty, some decay is due to the increased end effect (heat flowing down the metal extending from the heated length). In double-pipe test sections, the decay is due to decreased duty resulting from fouling. Additionally, the changing roughness of the surface and the thickness of the deposit can affect the velocity and shear stress in the test section. These changes in surface conditions tend to result in a decreased fouling rate and always result in the surface conditions being different from the starting surface conditions. To produce meaningful models and analysis, the assessed rate must be paired with the surface conditions corresponding to that rate. Because the reference point conditions are the best known fouling rate should be assessed as close to R_f = 0 and time =0 as possible.

Objective 4: Provides fouling rate on deposit rather than metal surface (most meaningful for translation to the field)

Initially, a fouling deposit grows on the bare test section surface. As the surface becomes fully covered (the end of the induction period), fouling growth transitions to deposition on deposit. In addition to the initial fouling rate, the induction period is another metric of interest [**8**]. The point at which the induction period ends is also subjectively determined based on the analyst's best judgment and influences how the initial fouling rate is assessed. The proposed method provides an objective method for assessment of the induction period.

Because the duration of an induction period of most field exchangers is negligible compared to the duration it operates with a fully covered surface, the rate of interest is the rate of fouling on deposit (not on bare metal). This criterion leads one to try to assess a rate away from R_f = 0 and time = 0 (as opposed to Objectives 2 and 3) and at resistances at which the surface is assumed to be fully covered.

CONSTANT DUTY VS CONSTANT WALL TEMPERATURE FOULING TESTS

During a fouling test, HTRI's crude oil fouling rigs are electrically heated and operated at a constant power. A common assumption for these rigs is that the surface conditions of the deposit are the same as those at the initial condition. This assumption is only true if true one-dimensional heat flow is achieved. In the HTRI test rigs, this is not the case due to the rig design. The electrical heating element is placed either inside or outside a tube. The test section length is the length that the electrical heater and tube are in contact. When heat is applied, the majority of heat will flow across the tube in this defined length; however, for very short test sections (L/D << 25), a non-trivial amount will be conducted down the tube extending from the heaters and into the fluid. This fraction of the duty is called the "end effect" and is a function of the length of the heated length, tube thickness, tube thermal conductivity, and convective heat transfer coefficient. For designs with heated lengths of 25-150 mm heated lengths (L/D 1-10), end effect of 5-40% would be expected under certain test conditions.

As fouling occurs, the deposit will primarily form in the heated length where the temperature is the hottest. As this occurs, the resistance to heat flow through the heated length increases thus diverting more heat down the extended tube and into the fluid. So although the test is run at constant power, the duty flowing through the heated length *is* decreasing and so is the surface temperature of the deposit.

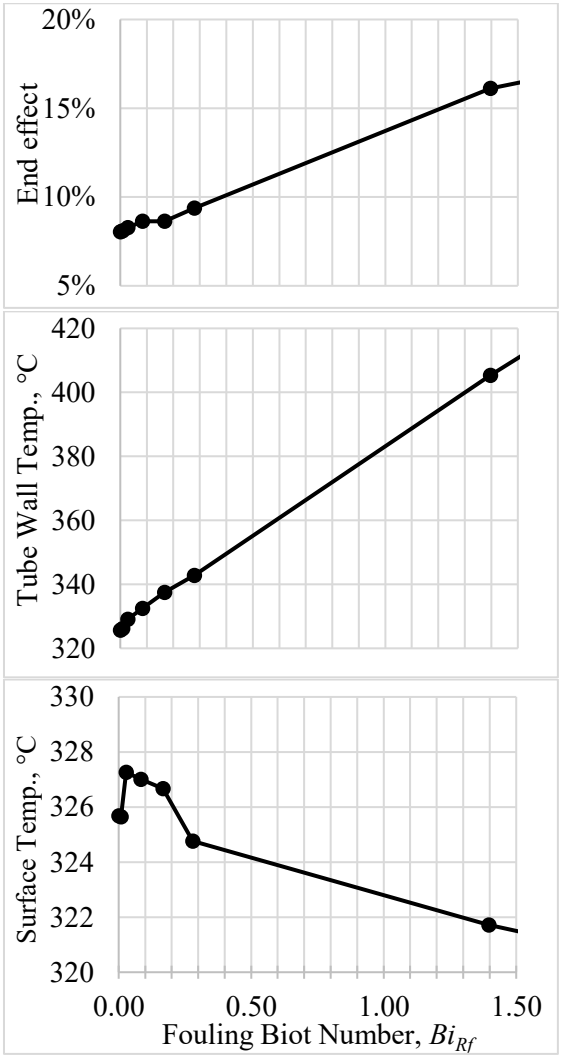

Fig. 2. End effect, wall temperature, and surface temperature trends with increasing fouling Biot number

To illustrate this behavior, HTRI used ANSYS FLUENT 14.0 to perform a parametric study in which a fouling resistance was applied in the heated length. The test section simulated had a tube of 12

ISBN: 978-0-9984188-1-0; Published online www.heatexchanger-fouling.com

mm ID and 22 mm OD with a heated length of 101 mm. A duty of 750 W was applied with a velocity of 2 m/s. Fluid properties of Duratherm HF were used. The resistance applied to the surface had no thickness so the impact of constriction is not present in the simulation (this would further increase end effect and decrease the surface temperature). The convective heat transfer coefficient for the clean condition was 2792 W/m^2 K. The resistances applied were 0, 3x10^{-6}, 10^{-5}, 3x10^{-5}, 6x10^{-5}, 10^{-4}, 5x10^{-4} m^2 K/W.

From Fig. 2 it is shown that end effect and wall temperature increase as fouling increases but the surface temperature of the deposit decreases. Further, this data clearly demonstrate that it is not possible to assume near constant surface temperature under constant heater duty for the HTRI test rigs. Based on this understanding, the primary driver in the reduction of the fouling rate in classic asymptotic type fouling trends is the surface temperature reduction which if there is sufficient fouling deposit may be combine with increased velocity and shear stress due to constriction.

RATE VS. RESISTANCE OBSERVATIONS

Due to the competing interests of Objectives 2 – 4, assessing the rate at a single point by applying a line of best fit or tangent (Fig. 1) along a fouling curve does not reasonably satisfy these criteria. These challenges are addressed using a trend in the data to assess the initial fouling rate. Fig. 3 is an example fouling resistance data obtained from the HTRI test rig, where beyond the induction period, the data follows the relationship proposed by Konak (1973) [**9**]:

$$\frac{dR_f}{dt} = K\left(R_\infty - R_f\right)^n \qquad (2)$$

Here, K and n are constants and R_∞ is the asymptotic resistance. When n = 1, Eq. 2 may be integrated with respect to time to obtain familiar Kern and Seaton equation [**10**].

For the test cases that exhibit the trend with rate vs. fouling resistance followed Eq. 2, a simplification was applied such that data at higher R_f values to be fit to a straight line [Eq. (3)]. The fit is then extrapolated backwards to determine the fouling rate at R_f = 0. This approach addresses Objectives 2 – 4. Extrapolating backward to R_f = 0 results in a rate more appropriately associated with initial conditions and at a point where the heat transfer coefficient has not changed relative to the reference point and is representative of growth on existing deposit. The y-intercept represented by b in Eq. (3) (y-intercept of the fit line in the bottom plot of Fig. 3) represents a fictitious point where the growth is on the existing deposit and R_f = 0.

$$\frac{dR_f}{dt} = m \cdot R_f + b \qquad (3)$$

Note: Direct fitting of Eq. (3) is not recommended; see Regression section.

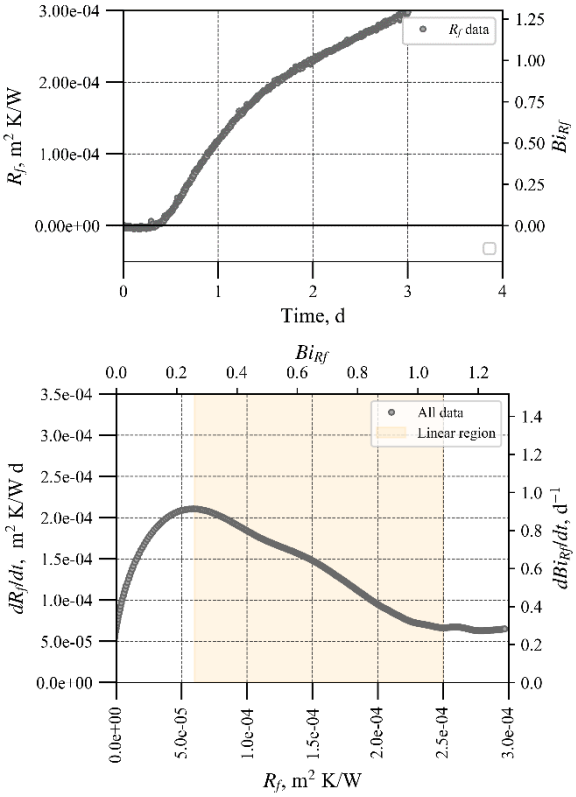

Fig. 3. (top) R_f vs. time for Test GRM873-1. (bottom) dR_f/dt vs. R_f for GRM873-1 with linear region highlighted.

DATA SELECTION CRITERIA

As Fig. 3 illustrates, most data sets include data at very low R_f values and sometimes at higher R_f values, where the trend with the fouling rate significantly deviates from linear. To be able to satisfy Objective 1, data-supported criteria have to define "low" and "high" R_f values so that non-linear portions of data are excluded from the analysis.

Poorly controlled test

Fluctuating operating conditions introduce artificial trends in the measured fouling resistance. Before fouling data can be analyzed, the operating conditions must be acceptably stable. The focus of this paper is on criteria for assessing the fouling rate. Eliminating "bad" data should occur prior to the algorithm framework presented here. Smith [**3**] provides guidance on fairly eliminating tests by setting limits on the standard deviation and the rate of change of operating conditions (e.g., bulk temperature, flow rate, test section power, and pressure).

ISBN: 978-0-9984188-1-0; Published online www.heatexchanger-fouling.com

Detection limit

The detection limit quantifies how variability in the operating conditions influences the heat transfer coefficient and how the fluctuation is perceived in terms of a fouling resistance. Quantifying a rig's detection limit is critical to accurate and effective data interpretation. The detection limit should be exceeded to ensure a meaningful change in the R_f. The maximum R_f should be more than ten times the detection limit.

The first step is to measure the variability (two standard deviations) for each operating condition (e.g., bulk temperature, power, and flow rate). The second step is to perform a propagation of uncertainty analysis on a single-phase heat transfer coefficient correlation using the measured variability of the operating conditions. Finally, the variation in h is translated into a variation in R_f using Eq. (1) and assuming no fouling; that is, $R_d = 0$. The resulting R_f uncertainty provides the resistance that must be exceeded for there to be a meaningful change in the overall heat transfer resistance. Values less than the detection limit may be due to fluctuations in operating conditions.

Deposit fully covering the surface

Using a confocal laser-scanning microscope, HTRI measures the roughness and thickness of the fouling deposits at the conclusion of each test. Directly quantifying surface coverage is not practical due to staining of the metal from the residual oil, so a fully covered surface is assumed when the deposit thickness exceeds (preferably more than twice) the core height of the bare metal surface. This is measured as the ISO surface roughness parameter, S_k (analogous to the line roughness value, R_k).

Assuming that deposit thermal conductivities range from that of the base crude up to values of 5 W/m K (coke) as aging occurs [**10**], the resulting deposit resistance, R_d, can be computed for an assumed thickness.

As shown in Fig. 4, for a thickness equal to $S_{k,metal}$, an R_d of 1e-4 m^2 K/W exceeds the resistance resulting from this deposit layer for all thermal conductivities in the range of crude and above. At a thickness of twice the $S_{k,metal}$, an R_d of 1e-4 m^2 K/W exceeds that of the deposit for k_d values greater than that of the crude oil.

In most cases, the h increases as fouling occurs; thus, the change in h typically has a negative contribution (i.e., $R_f < R_d$). Based on this analysis, full coverage for crude oil fouling is safely assumed when R_f > 1e-4 m^2 K/W. This threshold can be challenging to exceed in experimental tests, especially for milder test conditions, but it is generally achievable.

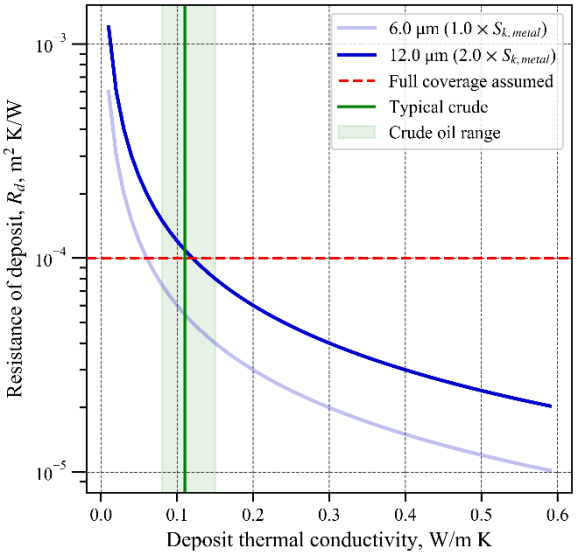

Fig. 4. Deposit resistance for assumed thickness over a range of deposit thermal conductivities.

The values shown here are specific to tubes HTRI uses for its fouling rigs and crude oil deposits. When a method is developed, the S_k of the test section's surface should be measured and reevaluated using thermal conductivities relevant to the test fluid/deposit.

Deposit resistance dominating the fouling resistance

Because changes in h impact the observed R_f, it is best to achieve and exceed an R_f value above which the deposit resistance, R_d, is the dominant contribution to the R_f value. Typically, h increases as fouling occurs; thus, $R_f < R_d$. The deposit resistance dominates when the ratio of R_f to R_d (β) is greater than 0.5 [Eq. (4)].

$$\beta = \frac{R_f}{R_d} > 0.5 \tag{4}$$

The heat transfer coefficient can be rewritten in terms of the relative increase of the initial value (α).

$$h = h_{ref} \cdot (1 + \alpha) \tag{5}$$

The fouling Biot number [Eq. (6)] is a useful way to interpret fouling resistance as it represents the change in thermal resistance due to fouling relative to the convective resistance at the reference point.

$$Bi_{Rf} = R_f \cdot h_{ref} \tag{6}$$

Because physical properties can vary from one test fluid to another, resulting in a wide range of heat transfer coefficients (convective resistances), a threshold defined in terms of a fouling Biot number,

ISBN: 978-0-9984188-1-0; Published online www.heatexchanger-fouling.com

Bi_{Rf}, is a criterion that may be more fairly applied to all tests.

Combining Equations (1) and (3) – (6) gives

$$Bi_{threshold} = \frac{\alpha}{(1+\alpha)} \cdot \frac{\beta}{(1-\beta)} \quad (7)$$

For a given value of β, Eq. (7) can be used to plot the threshold value for a given change in h (α), as shown in Fig. 5.

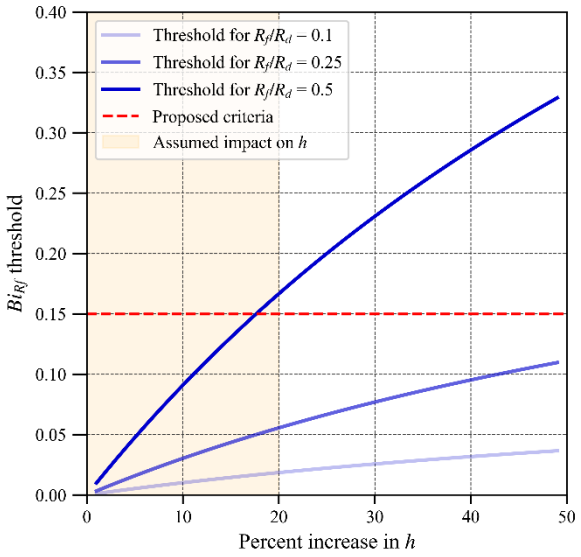

Fig. 5. Fouling Biot threshold above which R_f/R_d of 0.5, 0.25, and 0.1 for a given change in the clean h. The proposed analysis criterion is shown by the dashed line.

Based on sensitivity analysis of heat transfer correlations to changes in flow path area (deposit thickness), roughness, and surface temperature, in most cases, the variation of h usually does not increase by more than 20%. However, if a large increase in roughness occurs, h could increase well beyond 30%. Understanding and modeling the interaction between h and R_d is an ongoing area of research at HTRI.

For illustration, thresholds for β values of 0.1, 0.25, and 0.5 are shown in Fig. 5. For $Bi_{Rf} < 0.05$ in the figure, the discrepancy between R_f and R_d can be more than an order of magnitude ($\beta < 0.1$). As Bi_{Rf} in the range of 0.05 – 0.1 is achieved, the discrepancy can be significant, but the values of R_f and R_d are well within an order of magnitude of each other ($\beta > 0.25$).

A fouling Biot number threshold of 0.15 helps ensure that the observed trend is significantly impacted by R_d and not just fluctuations in h. A consequence of this criterion is that some tests with a clear trend that does not exceed this threshold will not be eligible for analysis. Future improvements to this criterion could use the deposit thickness and roughness of the resulting deposit to estimate the magnitude of impact on h (α) and then use Eq. (7) to set the threshold for each test. To avoid having data that do not meet the criteria for analysis, it is recommended to monitor R_f and Bi_{Rf} as the test is conducted and use the R_f and Bi_{Rf} thresholds to help decide if a test should be stopped or needs to continue.

No decay of surface conditions beyond the linear region

After the deposit growth has exceeded the thresholds, there comes a point where the dR_f/dt vs. R_f trend deviates from linear due to the surface conditions having decayed well away from the initial conditions such that the fouling rate stagnates at a much lower rate or goes to zero. Additionally, phenomena such as deposit removal and aging may begin to occur and are challenging to account for. Regardless of what causes the deviation from a linear trend, data beyond this point are highly uncertain and difficult to interpret and, were excluded from regression in this study.

Limit data beyond a given rate reduction. Although the surface conditions are not known, the change in fouling rate (dR_f/dt vs. time) is symptomatic of the surface conditions. As the deviation from the linear trend occurs after the rate has significantly decayed, excluding data based on the relative reduction in rate works well. This criterion was implemented by assessing the rate at the point of full coverage (i.e., 1e-4 m^2 K/W) and then multiplying by the percentage that represents the minimum rate allowed. Ideally, the reduction in rate would be relative to the initial fouling rate. However, such a criterion is a function of the output and leads to runtime and convergence issues. The rate evaluated at the point of full coverage is typically less than the initial fouling rate. HTRI determined that a value of 33% works well and means reduction of the rate relative to the initial rate is even less, indicating the surface conditions are likewise much different from the initial conditions. For example, if the rate at R_f = 1e-4 m^2 K/W is 3e-5 m^2 K/W d and, at a time of 10 days, the rate has reduced to 1e-5 m^2 K/W d, then rate analysis can exclude all data beyond a time of 10 days.

Limit data beyond an upper Bi_{Rf} threshold. In cases where high fouling rates are observed, the rate may not decay below the limit stated above or may accelerate until reaching a critical point at which an abrupt change in trend or a removal event may occur (a near vertical reduction in R_f). Data beyond such events are uncertain, and using an upper fouling Biot threshold may exclude them from analysis. Additionally, excluding higher fouling resistance data means that the trend is evaluated with more reliable data (*i.e.*, those closer to R_f = 0). The selection of the upper Biot threshold is somewhat arbitrary, and the exact value should not make a tremendous impact on the result. A value in the

ISBN: 978-0-9984188-1-0; Published online www.heatexchanger-fouling.com

range of 0.45 (three times the analysis limit of 0.15) to 1.0 is recommended.

FRAMEWORK FOR ALGORITHM

Per Objective 1, an algorithm implemented in code may be easily reused by others and is less susceptible to the corruption that can occur with spreadsheets over time. The purpose of this section is to provide guidance for researchers to development their own code to analyze the initial fouling rate.

Fig. 6 shows a simple, high-level diagram of HTRI's algorithm, consisting of three major steps: curve analysis, eligibility assessment, and regression.

Curve analysis

In the curve analysis step, the code reads in the time-series data and analyzes them to extract additional information. The results of curve analysis are then used in the following step to assess segments of data eligible to regress the R_f trend line [Eq. (8)]. The following evaluations are suggested:

- *Eliminate noise and smooth data*: Doing so helps highlight the underlying trend in the data and provides a data set more appropriate for assessing the first and second derivatives at each timestamp. A median filter works well for noise elimination. A Savitzky–Golay filter works well for smoothing and is available in many data-analysis programming languages like Python and MATLAB.
- *Assess first and second derivatives*: These two transformations provide the slope and concavity of the R_f curve, both of which are key values for application of criteria.
- *Digitize R_f, as well as first and second derivatives*: Assessing the sign of these values (arrays of **0**s and **1**s) easily identifies some useful metrics (e.g., percent of data with positive slope), forms a basis for eligibility assessment (e.g., negative slope = ineligible), and provides a means for the algorithm to detect oscillations (e.g., for day-night temperature fluctuations).
- *Extract timestamp information for key points of interest*: The timestamp, R_f, Bi_{Rf}, and fouling rate at key points reports not only meaningful statistics but allows useful application of the criteria in determining the eligible data subset:
  - Points at which Bi_{Rf} and R_f thresholds are crossed
  - Maximum R_f (not necessarily always the end point)
  - End of test
  - Point of highest rate (not always the first point)

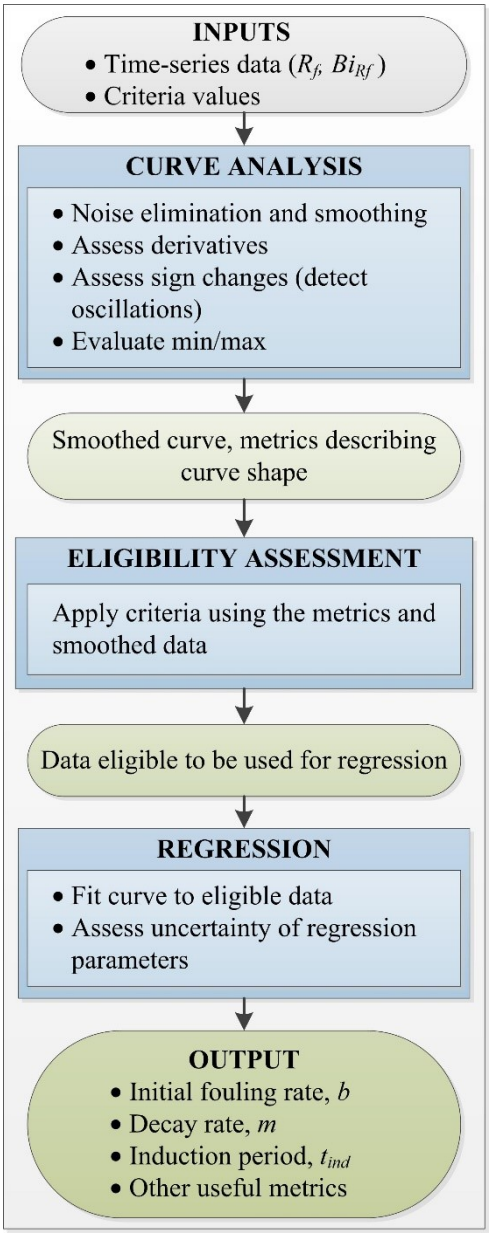

Fig. 6. Block flow diagram for fouling rate analysis algorithm.

Eligibility assessment

With all the values and metrics resulting from the curve analysis, criteria may be applied to create a data subset that may be reliably used to regress the R_f curve and assess the initial fouling rate.

The starting point for applying criteria based on R_f and the first and second derivatives is the digitized array for each; a **1** indicates that the value is eligible, and a **0** means the value is ineligible. Each time-series dimension can be considered independently, and criteria can be applied to identify eligible or ineligible segments. For example, data with R_f or Bi_{Rf} values above a maximum threshold would be forced ineligible (**0**) even though the sign is positive. Likewise, applied criteria can deem eligible short segments within otherwise ineligible

ISBN: 978-0-9984188-1-0; Published online www.heatexchanger-fouling.com

data sets, for example, those resulting from oscillations in 24-hour cycles.

After evaluation of the eligibility of R_f and the first and second derivatives, these arrays can be multiplied to produce a final eligibility array that is fed to the regression step. Fig. 7 shows eligibility for an example data set.

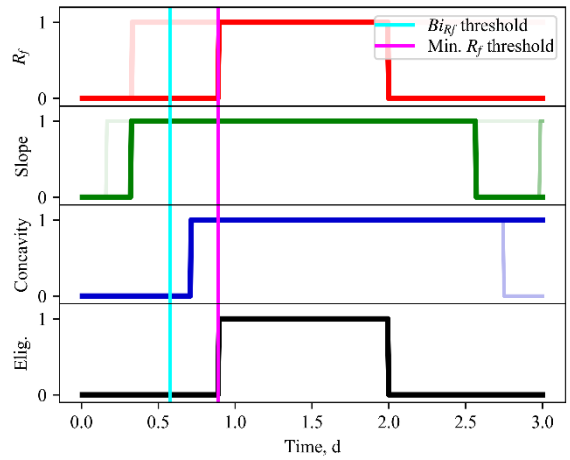

Fig. 7. Eligibility (**1** = eligible, **0** = ineligible) of data for GRM873-1. Bottom plot ('Elig.') is the multiplication of the "*Rf*", "Slope", and "Concavity" eligibility values.

Regression

The final step for an eligible data set is to regress a line to the data. Although the data exhibit a linear trend between the rate and the resistance, in practice it is *not* recommended to fit Eq. (3) to the data. The assessed rate is highly subject to how the data were smoothed and the derivative was taken.

A more robust approach is to integrate Eq. (3) with respect to time and fit the resulting equation [Eq. (7)] to the eligible R_f time series. It is recommended to use a regression tool that also reports the uncertainty of the regressed coefficients.

$$R_f = \frac{b\left(e^{m\cdot(t-t_{ind})}-1\right)}{m} \tag{8}$$

A decay rate plot (e.g., Fig. 8) with the overlaid linear trend line [Eq. (2)] is useful feedback in assessing the quality of the algorithm's result. The decay rate plot is created by first applying a smoothing function to the R_f vs t data and then using the smoothed data to assess the first derivate (dR_f/dt). The decay rate is then created by plotting the derivative versus the smoothed R_f data. As the details of the smoothing and derivatization can change the shape of the decay rate plot, eligible raw data was fitted to Eq. (7) instead of Equ. (2) which is the smoothed and first derivative data.

The result of regression is the three fit parameters b, t_{ind}, and m. The initial fouling rate, b, is the primary value of interest and per the applied criteria should always be positive. The induction period, t_{ind}, represents the time required for the surface to become fully covered. HTRI's algorithm does not constrain t_{ind} to be greater than zero (see Fig. 11 in Examples section); thus, when values across tests are analyzed, a negative value is interpreted as zero. The decay rate, m, represents the fractional change in rate per time. The decay rate is typically negative but in some cases has been positive (see Fig. 14 and Fig. 15 in Examples section). Based on this work, it is believed the primary driver causing a negative decay rate (rate decreases with increasing R_f) is the decrease in surface temperature and increase in velocity due to constriction when operated at constant flow rate. Increasing end effect, deposit growth, and roughing all play a role in decreasing the surface temperature and increasing shear stress. Interpretation of accelerating fouling rate trend (positive decay rate) is more challenging. Possible mechanisms that could cause an accelerating rate include: reduction in mass transfer limitations, generation of precursors may be increasing the rate, and decrease in thermal conductivity of each added layer due to decreased surface temperature. Regardless of the cause, for the HTRI test rig results the fluid and surface condition is migrating away from the initial condition, thus, extrapolation of the rate back to the initial condition is necessary.

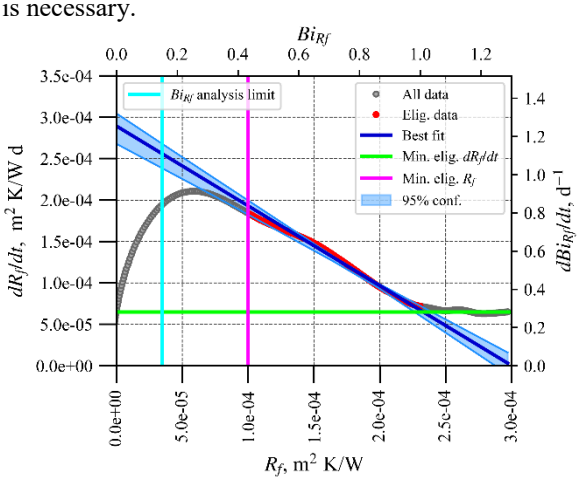

Fig. 8. Decay rate plot for Test GRM873-1(from Fig. 3) with overlaid thresholds and best-fit line.

EXAMPLES

The following example data were generated on HTRI's High Temperature Fouling Units #1 (HTFU-1) and #2 (HTFU-2). To provide context, Table I summarizes key design and operating information.

ISBN: 978-0-9984188-1-0; Published online www.heatexchanger-fouling.com

Table I. Summary of HTRI fouling rig specifications and operating information

Design/Operating Specification	HTFU-1	HTFU-2
Volume (L)	~40	~70
Number of test sections	2	4
Test section heated length	101 mm	
Test section ID	11.7 mm	
Heating mode during test	Constant duty	
Flow mode during test	Constant mass flowrate	
Recirculation	yes	
Turnover rate (vol./flowrate)	< 30 s, depends on flowrate	

The following graphs depict tests analyzed by the same algorithm but resulting in different trends. All data are shown in gray, with eligible data points overlaid in red. The best-fit line is shown in dark blue. The blue band is the 95% confidence interval of the best-fit line.

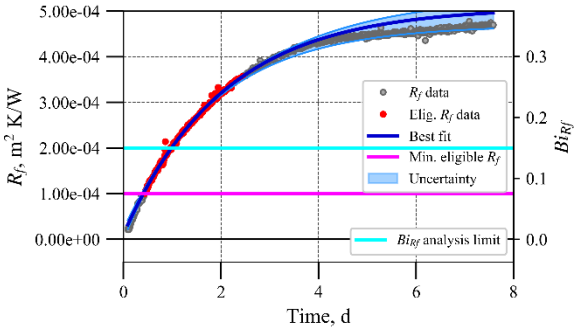

Fig. 9. A classic asymptotic fouling trend.

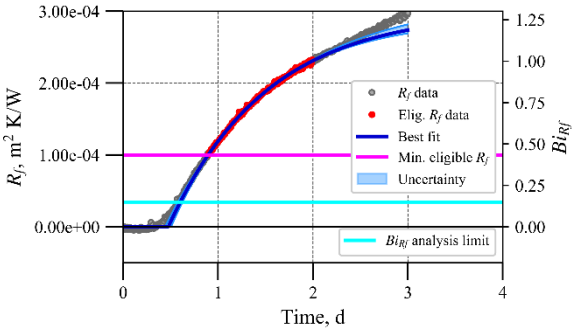

Fig. 10. Induction period followed by asymptotic trend (same data as shown in Fig. 3 and Fig. 8).

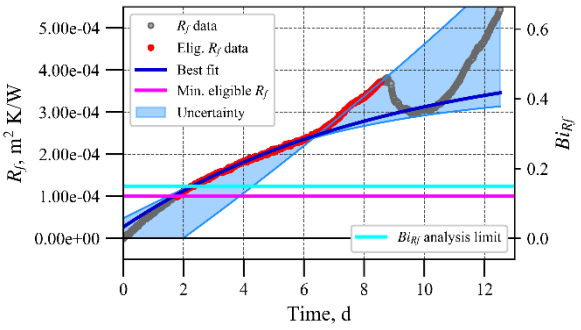

Fig. 11. Asymptotic trend followed by strange behavior at $Bi_{Rf} > 0.45$.

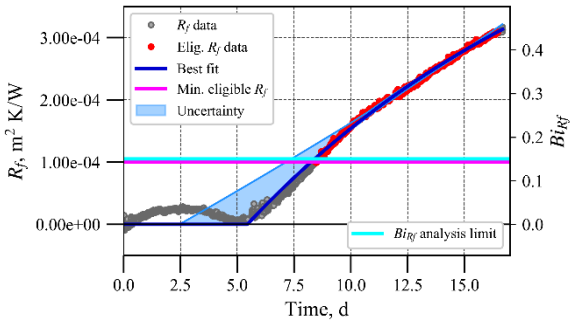

Fig. 12. Oscillations during induction period.

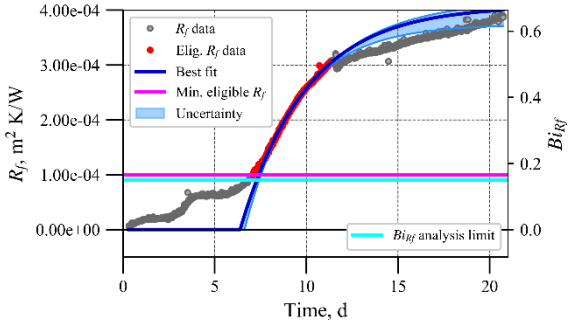

Fig. 13. Staggered induction period.

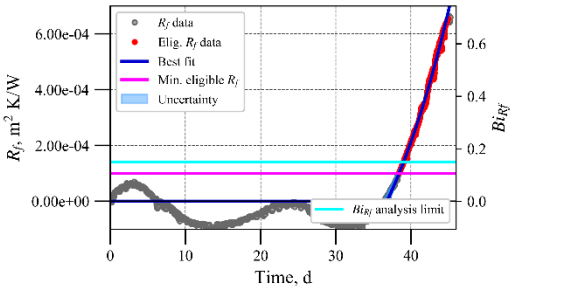

Fig. 14. Oscillations with negative R_f during induction period.

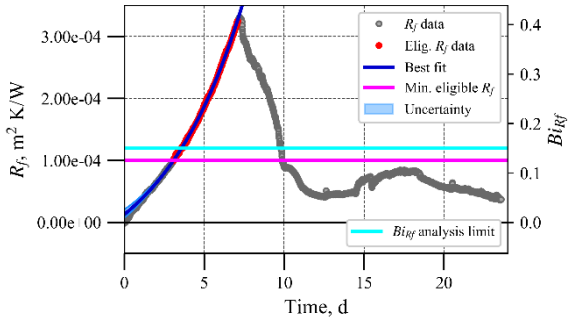

Fig. 15. Accelerating fouling trend (concave up).

DISCUSSION

Due to the amount of time and cost incurred for each test, most tests were only performed once. This restricts the study on adding error bars to the plots. Further studies are currently performed to understand the accelerating fouling trends (such as in Fig. 15). A consequence of the lower fouling thresholds is that tests that do not exceed these thresholds are not able to have the rate assessed. Criteria are needed to allow assessment of low-

ISBN: 978-0-9984188-1-0; Published online www.heatexchanger-fouling.com

fouling-rate trends that do not exceed the lower thresholds. Further, the thresholds and criteria used for rate analysis also provide guidance on for judging when to stop a fouling test.

CONCLUSIONS

Criteria-based analysis methods are essential for conducting rigorous and repeatable fouling research studies. In most HTRI experimental crude oil fouling data sets (> 85%), a linear trend in the fouling rate vs. fouling resistance is observed for data lying between a lower and upper threshold. This trend was used to extrapolate back to the point of no fouling resistance to determine the initial fouling rate.

HTRI has developed a method to address objectives for fouling rate analysis in its test rigs. This method provides a means for assessing the initial fouling rate, decay rate, and induction period that

- is representative of the fouling rate on deposit that is best associated with the initial test conditions
- is not influenced by the impact of a changing heat transfer coefficient

ACKNOWLEDGEMENTS

I'd like to acknowledge my fellow HTRI colleagues Edward Ishiyama, Jonathan Harris, and Matt Lane for their feedback and review of these ideas and this paper. I also appreciate the time and critical feedback provided by the peer reviewers.

NOMENCLATURE

b	initial fouling rate, m^2 K/W d
Bi_{Rf}	fouling Biot number
$Bi_{threshold}$	fouling Biot number threshold
dR_f/dt	fouling resistance rate, m^2 K/W d
d^2R_f/dt^2	second derivative of fouling resistance with respect to time
dBi_{Rf}/dt	Biot fouling rate, d^{-1}
h	heat transfer coefficient, W/m^2 K
k_d	thermal conductivity of the deposit, W/m K
m	decay rate, d^{-1}
R_d	deposit resistance, m^2 K/W
R_f	fouling resistance, m^2 K/W
R_k	line roughness parameter - core height of surface, m
S_k	surface roughness parameter - core height of surface, m
$S_{k,metal}$	surface roughness parameter - core height of surface metal, m
t	time, d
α	fractional increase in h_{ref}
β	ratio of R_f/R_d

Subscript

ind	induction period
ref	reference point

REFERENCES

1. Zaid S Saleh, R Sheikholeslami, and A P Watkinson, Fouling Characteristics of a Light Australian Crude Oil, in *Heat Exchanger Fouling and Cleaning: Fundamentals and Applications*, 1-8 (2003). [Online]. http://dc.engconfintl.org/heatexchanger/31
2. C. A. Bennett, S. Appleyard, M. Gough, R. P. Hohmann, H. M. Joshi, D. C. King, T. Y. Lam, T. M. Rudy, and S. E. Stomierowski, Industry-recommended procedures for experimental crude oil preheat fouling research, *Heat Transfer Engineering* **27**(9), 28 – 35 (2006).
3. A. D. Smith, Analysis of fouling rate and propensity for eight crude oil samples in annular test section., in *Proc. Heat Exchanger Fouling and Cleaning X*, 1 – 8, Budapest, Hungary (2013). [Online]. www.heatexchanger-fouling.com
4. A. D. Smith, E. M. Ishiyama, J. S. Harris, and M. R. Lane, Translating crude oil fouling testing rig data to the field: A road map for future research, in *Proc. Heat Exchanger Fouling and Cleaning XII*, 14 – 24, Aranjuez, Spain (2017). [Online]. www.heatexchanger-fouling.com
5. F Albert, W Augustin, and S Scholl, Roughness and constriction effects on heat transfer in crystallization fouling, *Chem. Eng. Sci.* **66**, 499-509 (2011).
6. Chao Shen, Yuan Wang, Zilong Zhao, Yiqiang Jiang, and Yang Yao, Decoupling analysis on the variations of liquid velocity and heat flux in the test of fouling thermal resistance, *International Journal of Heat and Mass Transfer* **123**, 227-238 (2018).
7. A. Ganguli, Heat transfer correlations for intube turbulent flow of liquids and gases, S-ST-1-1, Heat Transfer Research, Inc., Navasota, TX (1981).
8. M. Yang, A. Young, A. Niyetkaliyev, and B. Crittenden, Modelling the fouling induction period, in *Proc. Heat Exchanger Fouling and Cleaning VIII*, 69 – 75, Schladming, Austria (2009). [Online]. www.heatexchanger-fouling.com
9. A. R. Konak, Prediction of Fouling Curves in Heat Transfer Equipment, *Trans. Instn Chem. Engrs.* **51** (1973).
10. E. M. Ishiyama, F. Coletti, S. Macchietto, W. R. Paterson, and D. I. Wilson, Impact of deposit ageing on thermal fouling: Lumped parameter model, *AIChE Journal* **56**(2), 531 – 545 (2010).

ISBN: 978-0-9984188-1-0; Published online www.heatexchanger-fouling.com